FINITE ELEMENT ANALYSIS OF WOOD ADHESIVE JOINTS

Thomas GEREKE[*]
Technische Universität Dresden
Institute of Textile Machinery and High Performance Material Technology
Hohe Str. 6, 01069 Dresden, Germany
E-mail: thomas.gereke@tu-dresden.de phone +49 351 46342244, fax +49 351 46334026

Stefan HERING
ETH Zurich, Institute for Building Materials
Stefano-Franscini-Platz 3, 8093 Zurich, Switzerland

Peter NIEMZ
Bern University of Applied Sciences
Solothurnstrasse 102
E-mail: peter.niemz@bfh.ch, phone: +41323440264
Formerly (retired march 2015):
ETH Zurich, Institute for Building Materials
Stefano-Franscini-Platz 3, 8093 Zurich, Switzerland
E-mail: niemzp@retired.ethz.ch

Abstract:
Engineered wood products such as glulam or cross-laminated timber are widely established in the construction industry. Their structural behaviour and reliability clearly bases on the adhesive bonding. In order to understand and improve the performance of glued wood members a finite element modelling of standard single lap shear samples was carried out. A three-dimensional model of a longitudinal tensile-shear specimen with quasi-centric load application was developed. The main influences of wood and adhesive parameters on structural performance were identified. Therefore, variations of the elasticity, the annual ring angle, fibre angle, and the interface zone and their effect on the occurring stresses in the adhesive bond line were investigated numerically. The adhesive bond line is most significantly sensitive to the Young´s modulus of the adhesive itself. A variation of the fibre angle of the glued members in the standard test is an essential criterion and to be considered when preparing lap shear specimens. A model with representation of early- and latewood gives a more detailed insight into wooden adhesive joints.

Key words: adhesive bond line; finite element model; mechanical properties; single lap shear sample.

INTRODUCTION

Engineered wood products such as glulam or CLT (cross-laminated timber) are widely established in the construction industry. Their structural behaviour and reliability clearly bases on the adhesive joints. A modelling framework for glued wooden joints would be desirable in order to understand and improve the performance of glued wood members. Such is the goal of this study.

Basic issues concerning the constitutive laws of wood are e. g. presented by Ranta-Maunus (1975) and Bazant (1985). The direct modelling of different material properties such as orthotropic elasticity, swelling and shrinkage and certain creep properties are described in Hanhijärvi (1995); Kaliske and Rothert (1997); Liu (1993); Liu (1994); Martensson (1994); Ormarsson et al. (1998); Ormarsson (1999). Further publications cover concrete applications, e. g. Becker (2002), or consider moisture effects Svensson and Toratti (2002). Further modelling aspects deal with special issues or applications, whose results could be considered for special problems, e. g. Chassagne et al. (2005); Dubois et al. (2005); Fortino et al. (2009); Gereke (2009); Gereke and Niemz (2010); Gereke et al. (2010); Moutee et al. (2005). Due to the large variety of modelling options, the approaches used and the available software can usually be resorted to certain parts of the existing publications only. Thus, often own extensions to the implementations and the algorithms have to be executed.

The natural material wood with microscopic and macroscopic properties is especially challenging for the implementation into material models. It exhibits anisotropic, inhomogeneous and non-linear material behaviour with distinct dependencies to different influencing factors. Different modelling approaches exist, e. g. Becker (2002); Gereke (2009); Grimsel (1999); Hanhijärvi (1995);

---

[*] Corresponding author

Ormarsson (1999); Serrano (2000), which differ in the choice of the constitutive components and the grade of approximation and often follow a specific topic.

Starting with investigations of the influence of various parameters on the mechanical loading of the adhesive joint in the tensile-shear test, an orthotropic-elastic material model is introduced. Through a variation of important parameters it is shown, which influence single parameters have on the loading of the glue line and thus on the demands onto the applied adhesive. Finally, findings are summarized and their influence on the simulation of adhesive bond lines and their loading are evaluated.

For the determination of properties of glued wood under consideration of varying parameters of the materials and the gluing, standardized tensile-shear tests according to EN 302 (2004) are used. They secure comparability of the results and of the tested materials and provide an elementary data basis for further investigations.

For the improvement and examination of the applied testing method and for the analysis of the occurring stresses in the adhesive joint under variation of relevant parameters numerical investigations of the tensile-shear tests have been performed. Gindl-Altmutter et al. Gindl-Altmutter et al. (2012) found a good agreement between apparent shear strength and a stress concentration factor derived from a model by means of Volkersen's equation for lap-shear specimens of varying geometry. In experimental tests and numerical modelling Müller et al. Müller et al. (2005) showed that in a lap joint experiment the material close to the edge of the adhesive bond line is highly strained.

The simulation of deformations and stresses in the tensile-shear test was conducted for thick single lap-shear adhesive bonds by Koch (1996) and for two-dimensional models of the standard specimens by Zink et al. (1996). Serrano Serrano (2004) presented simulation results of the post-peak behaviour of the tensile-shear test with a three-dimensional model. He investigated the influence of eccentric loading with three different adhesive variants and confirmed the influence of the adherend on the occurring stresses, which are further investigated in the following.

MATERIAL AND METHODS
Homogeneous model

Opposite to previous works of Koch (1996) and Zink et al. (1996) a three-dimensional model of a longitudinal tensile-shear specimen with quasi-centric load application was developed. The geometry is oriented at the standard EN 302 (2004) and is displayed in Fig. 1 with the respective finite element discretization. In order to improve the local mesh resolution the number of elements was increased at the bond line. The choice of a kinematically compliant element geometry and a processible number of elements was challenging due to the small thickness of the bond line. It has been realised with ten solid elements in the thickness direction and a maximum ratio of the cuboid dimensions of ≤ 10. Eight-node solid brick elements with a linear approach in the displacements were used. The boundary nodes at the top and bottom of the modelled bond line were connected by displacement constraints to the respective adherends. For the model of the standard tensile-shear test a restraint at the lower end of the specimen and a laminar loading at the upper side of the specimen was chosen as boundary conditions.
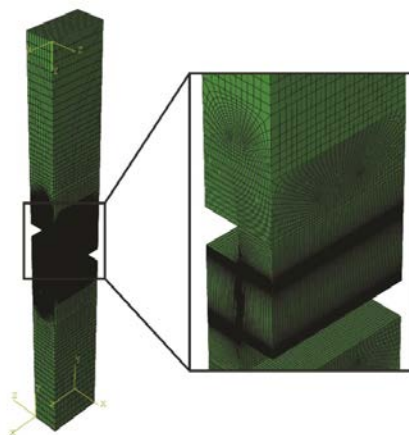

Fig. 1.
Discretized shear tension specimen.

A linear-elastic material behaviour was used. The material of the adherends was implemented as orthotropic with the mechanical properties of beech wood (*Fagus sylvatica* L.) as presented in

Table 1. The adhesive joint was modelled as isotropic material with a Young's modulus of E_{adh} = 470 MPa and a Poison ratio of v_{adh} = 0.3, which corresponds to one component polyurethane as measured by Konnerth et al. (2007b).

Table 1

Elastic constants of beech wood at standard climatic conditions used in the study Hering et al. (2012) (average moisture content 12.5 %)

Young's moduli [MPa]	E_L	13900
	E_R	1900
	E_T	606
Shear moduli [MPa]	G_{LR}	1280
	G_{LT}	855
	G_{RT}	486
Poisson ratios [-]	v_{TR}	0.64
	v_{TL}	0.24
	v_{RL}	0.27
	v_{RT}	0.27
	v_{LR}	0.07
	v_{LT}	0.09

Inhomogeneous model

A more detailed model was created where early- and latewood are represented numerically with four annual rings (Fig. 2). The early- and latewood zones are arranged concurrently and staggered, respectively, between both wood parts. The properties of the components of the annual ring were taken from Keunecke et al. (2008) for Norway spruce as follows:

- mean density wood $\overline{\rho}_{wood} = 480\ kg\ m^{-3}$

- mean density earlywood $\rho_{EW} = 275\ kg\ m^{-3}$

- mean density latewood $\rho_{LW} = 1050\ kg\ m^{-3}$

- volume fraction earlywood $\varphi_{EW} = 0.25$

Young's and shear moduli are scaled accordingly with the rule of mixture in order to account for the lower/ higher density of early-/ latewood. Poisson ratio is kept constant compared to the homogeneous model.
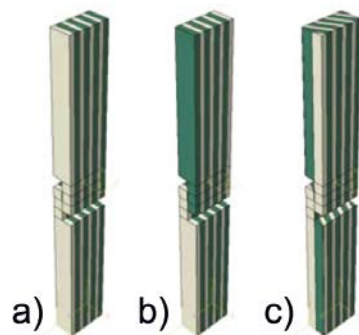

Fig. 2.
The shear-tension sample modelled with early - and latewood: a) concurrent array, annual ring angle $\theta = 0°$, b) staggered array, $\theta = 0°$, c) concurrent array, $\theta = 30°$.

Experimental tests

To assess the quality of the numerical simulation actual and numerical experiments are carried out under identical conditions. The resulting comparison of the two methods is used for the validation

ONLINE ISSN 2069-7430
ISSN-L 1841-4737

PRO LIGNO
www.proligno.ro

Vol. 12 N° 1 2016
pp. 3-14

of the computer-based prediction method. For the determination of comparable data, tensile-shear specimens according to EN 302 (2004) were sprayed with a speckle pattern in the areas of interest, see Keunecke et al. (2008). During the standard test the lateral side of the specimen was observed by a distortion-free CCD camera (*charged-coupled device*). The resulting image sequence was then analysed with a cross-correlation algorithm in the software VIC 2D (Correlated Solutions, USA).

RESULTS AND DISCUSSION
Model validation
The experimental and numerical obtained shear deformations at identical loadings along a path in the centre of the specimen are compared in Fig. 3. Despite small differences at the boundary areas the comparison of empirical and theoretical obtained data reveals a good correlation. Numerical calculations and actual tests correlate in their curve progression and the absolute values. However, due to measurement reasons the strain distribution could not be detected over the entire sample in the experiments. The advantage of the numerical simulation is that it yields the altered strain distribution within the adhesive joint as well. At the same time, the adhesive joint that is non-resolvable in the experiments is characterized by a steady course of the experimental shear strain distribution.

Fig. 4 presents the significant shear stresses within the adhesive using the homogenized model for the simulation. Due to the specimen geometry a point symmetry around the dimensional centre-point occurs. Perpendicular to the load direction an additional axis symmetry of the shear stresses exists. Those symmetries occur only at symmetric material directions of the top and bottom layers.
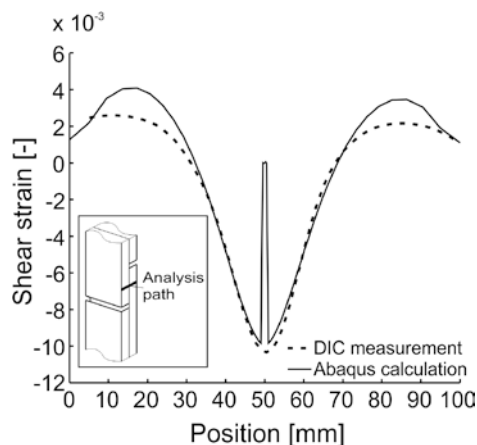

Fig. 3.
Comparison of shear strain in actual and numerical tensile-shear tests along the thickness of the specimen.
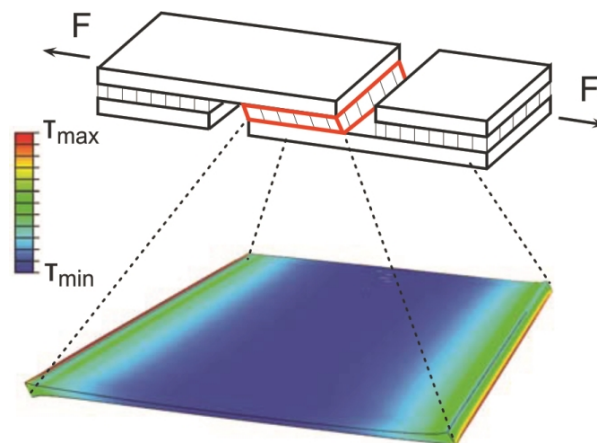

Fig. 4.
Exemplary shear stress distribution within the adhesive joint in a shear-tensile test.

Sensitivity analyses
In the following sections fundamentals for changing the stress on the adhesive joint will be developed by varying different parameters in the homogeneous model. For quantifying the loadings on the joint, paths denoted A, B and C as illustrated in Fig. 5 are analysed. The Young's modulus of the adherends in the loading direction and the Young's modulus of the adhesive are varied. The influence of the material principal directions is studied through a variation of the annual ring angle in the RT-plane of samples for discussion of different test conditions. Furthermore, the influence of an interface area between the adhesive and the wood is detected in the numerical simulation using a variation in rigidity of this intermediate layer. The purpose of this computational study is the evaluation of the impact of the above factors in relation to the type, the size and the sensitivity to the calculated stress and strain gradients, respectively. For this purpose, the influence of randomly occurring variations and the effect of specific changes in parameters during tensile-shear testing under a load of 10N per 1mm^2 bond area is determined.
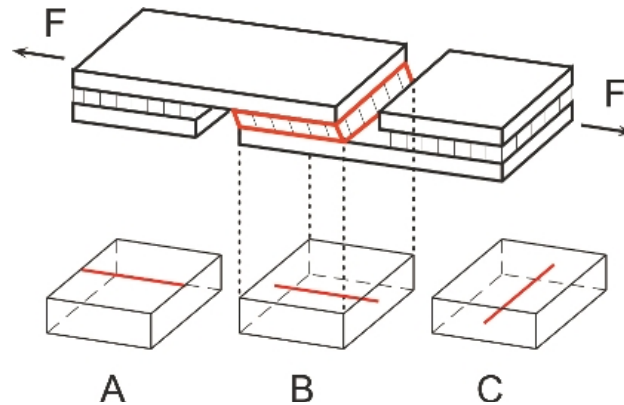
ONLINE ISSN 2069-7430
ISSN-L 1841-4737

PRO LIGNO
www.proligno.ro

Vol. 12 N° 1 2016
pp. 3-14

Fig. 5.
Sketch of the applied stress and strain paths in the adhesive joint of a tensile-shear specimen.

Elasticity of the adhesive

Fig. 6 shows the normal stress component σ_{11} along path A. It is oriented normal to the glued area and denoted peel stress. It is the main component in the delamination processes. It takes extreme values at the edges where also the largest differences of the parameter study of varying Young's moduli of the adhesive can be observed. Due to this effect boundary areas are magnified in this and other diagrams. It is been refrained from a quantitative evaluation of the absolute values at the edges, since numerical factors such as the mesh density, the shape function and material model induced peaks through not considered viscous effects may play a significant role. Especially at the boundaries between two materials those factors are hard to control and their effect is not readily interpretable. Thus, analyses of paths B and C were conducted.

The shear stress distribution along path C in Fig. 7 shows a symmetrical behaviour with significantly lower edge and absolute values. This is caused on the one hand by the path that is aligned perpendicular to the loading direction and centred in the adhesive joint and on the other hand by the other stress component. Under these conditions the shear stress distribution is approximately constant over the bond line width. In contrast, the shear strain ε_{12} shows a pronounced concave profile in the middle of the adhesive joint in the direction of loading with the expected vanishing distortion at the free edges and the module-proportional absolute values in the central part of the adhesive joint (Fig. 8b). The corresponding shear stresses τ_{12} in Fig. 8a, however, show the expected equal levels with differences in the peripheral and central region. With increasing elasticity of the adhesive, the ratio of maximum stress near the edge to minimum stress in the centre increases. The visible differences in the occurring maximum values are as remarkable as the low boundary condition-induced deviation from symmetry.
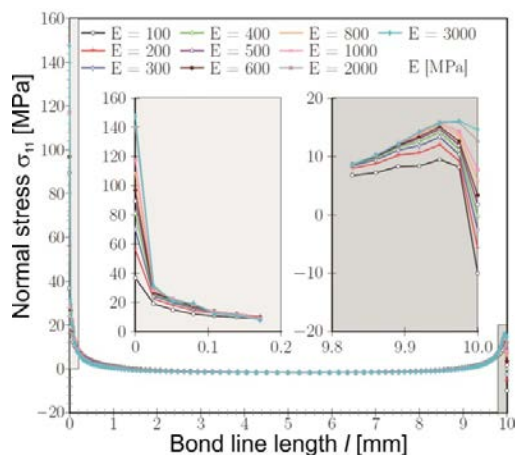

Fig. 6.
Normal stress σ_{11} along path A between the adhesive and wood under variation of the elasticity of the adhesive.
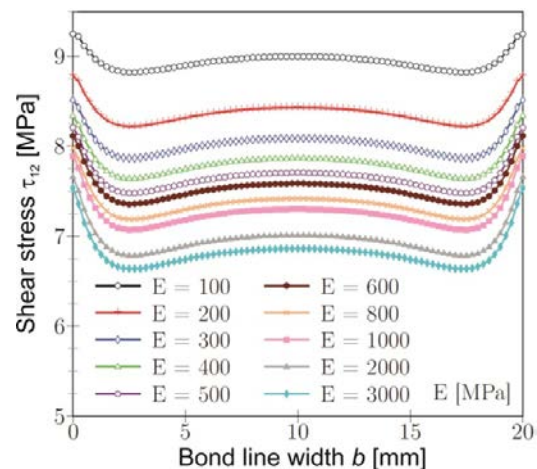

Fig. 7.
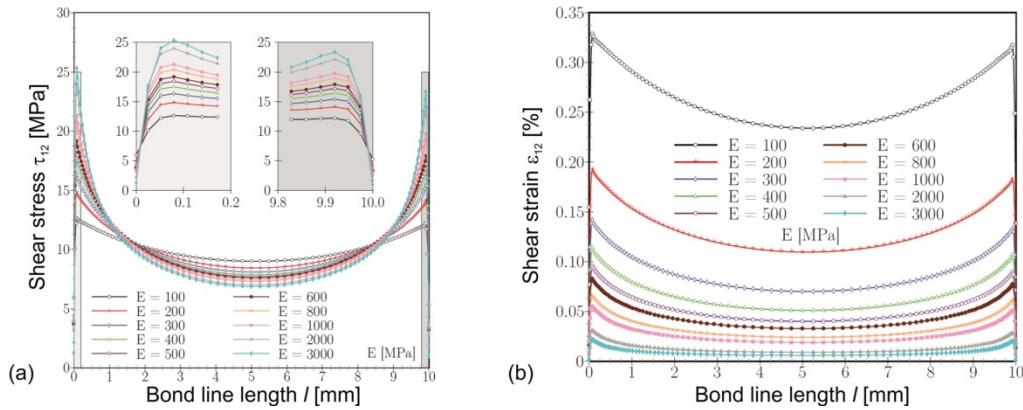*Shear stress τ_{12} along path C under variation of the elasticity of the adhesive.*

Fig. 8.
Shear stress (a) and strain (b) distribution along path B under variation of the elasticity of the adhesive.

Elasticity of the adherend

The effect of the material properties of wood on the loading of the glue joint in the shear tension mode is determined by evaluating the influence of the longitudinal modulus of wood, E_L. Fig. 9 shows the shear stress distribution over the glue line length along path B with values E_L = 8000…20000MPa. As can be seen from the Fig. a higher wood modulus yields a reduction of the shear stress in the adhesive bond line. In contrast to the previous considerations, the shear strain ε_{12} follows the shear stress distribution at a uniform level.
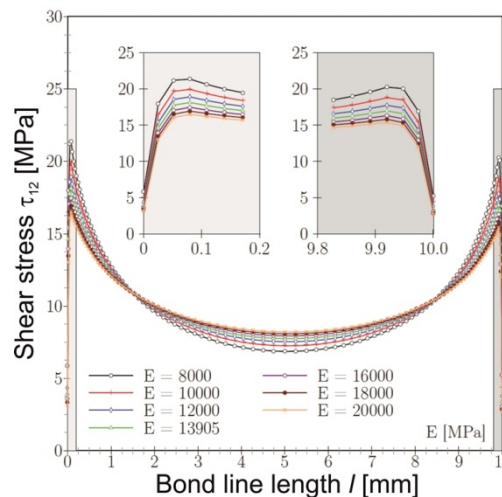

Fig. 9.
Shear stress τ_{12} along path B under variation of the elasticity of the adherend.

Variation of the annual ring angle θ

The sensitivity of the tensile-shear test to a manufacturing-induced variation, i. e. an inaccuracy in the annual ring angle, is investigated here. Due to the orthotropic nature of wood a small change in the orientation could have a great effect on the mechanical response. Model calculations were performed with a mutual mirrored annual ring orientation within both wood parts as illustrated in Fig. 10. Shear stress in path B is shown in Fig. 10 for seven steps of the angle θ. The maximum value differs around 2MPa, whereas horizontal annual rings (θ = 90°) stress the adhesive bond the most. In identical annual ring orientations on both sides (results not shown here) an additional moment occurs, which is small in its value but could be responsible for a potential point of failure or preferred direction of failure.
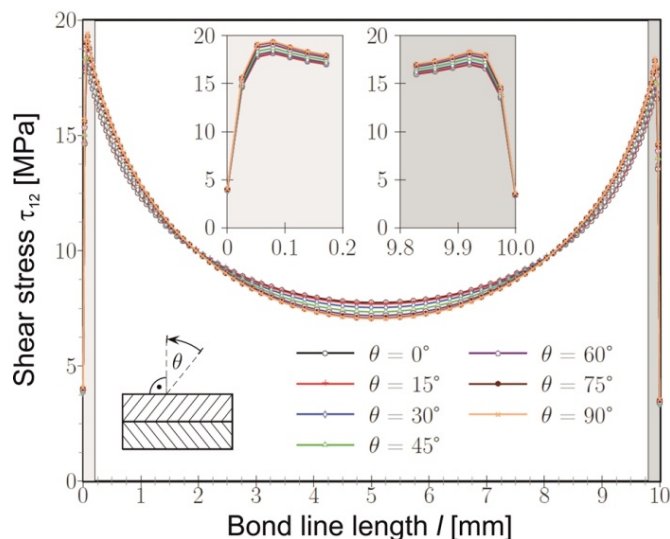
ONLINE ISSN 2069-7430
ISSN-L 1841-4737

PRO LIGNO
www.proligno.ro

Vol. 12 N° 1 2016
pp. 3-14

Fig. 10.
Shear stress τ_{12} along path B under variation of the annual ring angle of the adherends.

Variation of the fibre angle α

αIn the preparation of specimens for tensile-shear tests, variations in the fibre angle can occur in the test object. To assess this influence on the stress of the adhesive joint the possibilities of fibre angle arrangement shown in Fig. 11 were varied between $\alpha = 0°$ … 15° in steps of 5°. Type I and type II were grouped together, because the fibre angles of the two variants only differ in sign. The shear stress distribution along path B is shown in Fig. 12a. The variants of type I differ fairly strong in their absolute values of the shear stresses on both edges. They range from ≈ 18 to 27MPa at the most stressed point at an angle variation by only 15°. However, by varying the fibre angle α in the type II configuration, the maximum values are between ≈ 16 to 18MPa, which lie in their spread well below the values of type I. This phenomenon is known from practice and is attributed to the type of fibre arrangement in the shear-tension test. Relative to the loading direction the fibres run in the direction of the bonded joint (type I). Thus, greater stress and lower strength than in type II configuration are the result, where fibres move away from the joint under loading. Results of the stress in the type III configuration confirm this fact. It was experimentally observed already by Furuno et al. Furuno et al. (1983). According to the two different fibre orientations shear stresses in the adhesive joint are accordingly excessive or almost unchanged.
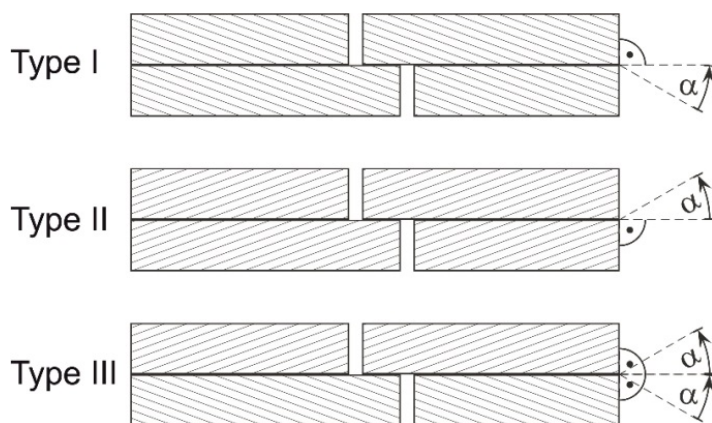

Fig. 11.
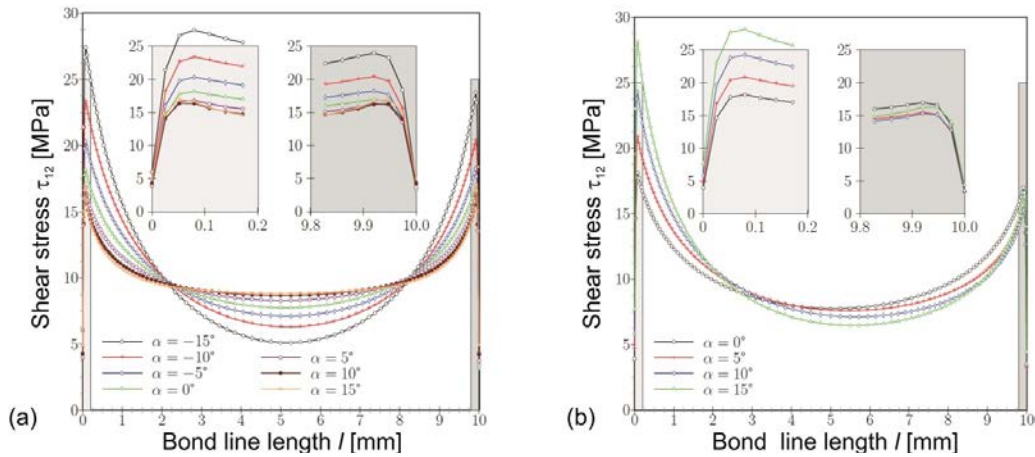*Sketch of the three types of fibre angle configurations.*

Fig. 12.
Shear stress τ_{12} along path B under variation of the fibre angle for a) type I and type II and b) type III configurations.

Interface zone

The description and modelling of adhesive joints can be carried out in different ways. Mainly solid elements are used for the simulation of the occurring stresses or cohesive elements are used for the simulation of bond failure. Slid elements allow the simulation of the stress and strain distribution within the adhesive. However, a geometric resolution to the cell level is limited. Since the adhesive can penetrate into the wood micro structure depending on the chosen material and process parameters Hass et al. (2012), the material properties of this mixing zone can be changed Konnerth et al. (2007a). In order to assess the effect of this mixing zone on the adhesive joint, an interface zone with half the adhesive thickness was implemented on both sides of the adhesive zone in the model. Although the penetration depth of the adhesive depends on the material combination, this general description was used to get a first impression of the interface impact on the model performance. The interface zone was modelled with four elements in the thickness direction and geometrically within the wood part of the sample. Fig. 13 shows the location and the proportions of the tensile-shear sample, the interface zone and the adhesive joint. The stiffness of the interface zone was varied in terms of the three Young's moduli and three shear moduli with increments of E_i^*, G_i^* = 0.75, 1.00, 1.25, and 1.50 E_i, G_i. Poisson ratios were not varied. The results of the shear stress along path C are displayed in Fig. 14. The calculated differences are very small in relation to the used variation of input variables. The stress paths are in the same order of magnitude and feature the same characteristic trend. It is noteworthy that with increasing stiffness of the interface zone shear stress decrease but increase at the highest variation. Basically the calculated loading of the adhesive joint through the integration of an interface zone with varying stiffness is negligible. However, the influence on the strength of the connection cannot be judged and may be significant.
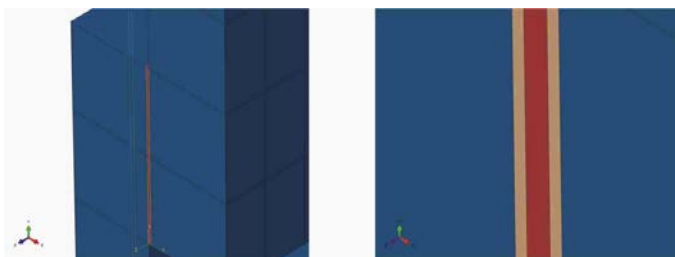

Fig. 13.
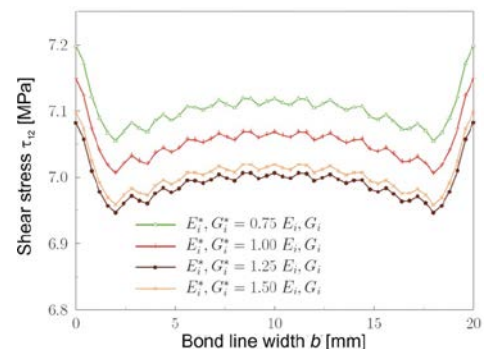*Model of the adhesive joint with integrated interface zone.*

Fig. 14.
Shear stress τ_{12} along path C under variation of the stiffness E_i^* and G_i^* of the interface zone.

Sensitivity analysis

For a quantifiable assessment of the previously presented variations of the typical tensile-shear test with beech wood and its effect on the stress of the adhesive joint, a sensitivity analysis was performed. The presented variations of the elasticity, the annual ring angle, the fibre angle, and the rigidity of the interface zone and their effect on the maximum occurring stress in chosen analysis paths are summarized in Table 2. The maximum and minimum values of the parameter studies at the most stressed point of the respective analysis path are displayed. To this statement the ratio of the maximum to minimum value was added, to obtain a relative scaling of the difference occurring in the corresponding parameter variation. Based on this ratio, it is possible to gain an impression of the sensitivity of the input parameter on the highest stress values in the adhesive bond. The variation of the elasticity is handled using the variation of the Young's moduli of the adhesive and the adherend. It is readily appreciated that the chosen variation range for the adhesive moduli has the greatest influence on the stress in the joint. This is expressed especially in paths A and B with the data of path B as the most significant, because in path A numerical peaks play an important role and no global maximum stresses occur in path C. The influence of the variation of the annual ring angle on the stress of the adhesive joint due is comparatively low due to the lower absolute values. A variation of the fibre angle, however, is as a decisive criterion always to be considered, which is significantly shown by the large ratios of maximum to minimum values. In addition, it can be conducted, what influence the fibre orientation based on the bond line can have in terms of bond line stress, which clearly confirms the experimental observations of Furuno et al. Furuno et al. (1983). A stiffness variation of a fictive interface zone, however, has a relatively small influence on the stress within the adhesive joint.

Table 2

Sensitivity analysis: Effect of the parameter variation on the maximum and minimum stress values and their ratio

Parameter	Variation range	Stress component	Analysis path	Max value [MPa]	Min value [MPa]	Max/Min [-]
Elasticity of adhesive	100…3000 MPa	Normal stress	A	147.5	36.9	4.0
		Shear stress	B	25.3	12.6	2.0
		Shear stress	C	9.2	7.5	1.2
Elasticity of adherend	8000…20000 MPa	Shear stress	B	20.6	16.2	1.3
Annual ring angle	0…90°	Shear stress	B	19.4	18.2	1.1
		Shear stress	C	8.2	7.2	1.1
Fibre angle type I	-15°…0°	Shear stress	B	27.4	18.2	1.5
			C	8.2	5.0	1.6
Fibre angle type II	0°…15°	Shear stress	B	18.2	16.4	1.1
			C	9.7	8.2	1.2
Fibre angle type III	0°…15°	Shear stress	B	28.1	18.2	1.5
			C	8.2	7.2	1.1
Interface zone	0.75…1.5 x 13900 MPa	Shear stress	C	7.2	7.1	1.014

Inhomogeneous model

A more detailed model of the tensile-shear test considers the difference in density and, thus, mechanical properties of early- and latewood and is denoted inhomogeneous model here. The shear stress distribution within the adhesive joint, where the wood was modelled with the inhomogeneous approach, is shown in Fig. 15. Stress peaks occur at the edges and at the interface between early- and latewood due to significant stiffness differences.

Figures 16a and 16b present the shear stress in path C for the concurrent and staggered arrays, respectively, under a variation of the annual ring orientation, θ, from 0° to 90°. The curves for $\theta = 0°$ are flat compared to others which alternate along the bond line width around a mean value. Stress peaks are due to transition between areas of different stiffness, i. e., earlywood and latewood. At a 90° orientation no transition between different wood layers occurs and thus the stress curve in the glue line is smooth. The ratio of maximum to minimum stress is larger for the concurrent array than for

ONLINE ISSN 2069-7430
ISSN-L 1841-4737

PRO LIGNO
www.proligno.ro

Vol. 12 N° 1 2016
pp. 3-14

the staggered array since the transition between early- and latewood is the same on both sides of the adhesive and stiffness difference are less balanced as in the staggered configuration.
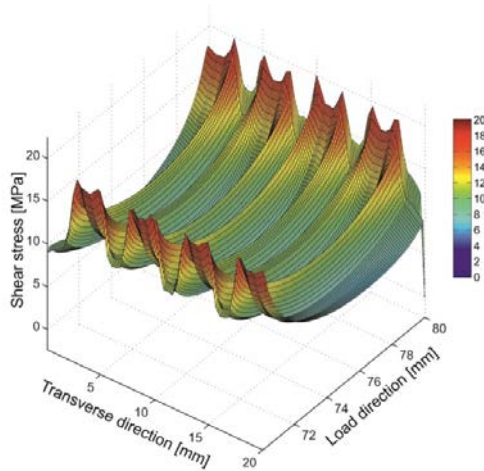

Fig. 15.
Shear stress within the adhesive joint under consideration of early- and latewood (inhomogeneous model) with material data of spruce wood by Keunecke et al. (2008).
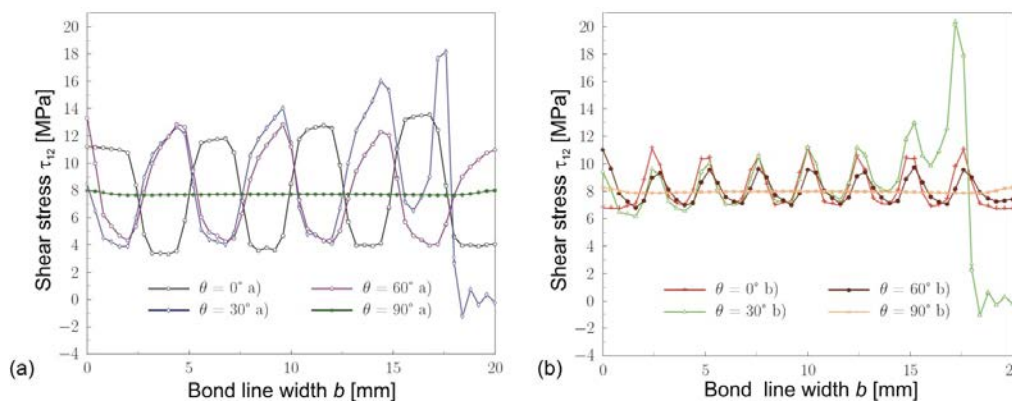

Fig. 16.
Shear stress τ_{12} along path C under variation of t under consideration of early- and latewood (inhomogeneous model) with varying annual ring orientations θ for a) concurrent array and b) staggered array.

CONCLUSIONS

The stress distribution within an adhesive bond line in a single lap shear test was investigated by means of numerical simulations. In a sensitivity analysis the influencing factors stiffness of the adhesive and the wood, annual ring and fibre orientation of the wood, and the stiffness of the interface zone were studied. Significant influences of the adhesive modulus were detected. Thus, the choice of the adhesive clearly determines the stiffness of the joint. A variation of the annual ring angle has a minor effect on the stress in the adhesive bond. However, angle variations could induce asymmetric stress distributions, which influences the fracture and crack initiation. Adhesion with mirrored annual ring layers between upper and lower lamella with vertical growth rings ($\theta = 0°$) may increase the reproducibility and minimize occurring variations and are therefore recommended. A variation of the fibre angle is an essential criterion and to be considered when preparing lap shear specimens. A fictive interface zone has a negligible effect on the stress distribution, but could affect the bond strength, which was not investigated here. Density differences between early and latewood have a clear influence on the adhesive bond. Further investigations on plastic deformations and bond failure could lead to a more detailed numerical description of adhesive bond lines. Integration of the interface zone into numerical failure analyses may be of importance.

ACKNOWLEDGEMENTS

REFERENCES

Bazant ZP (1985) Constitutive equation of wood at variable humidity and temperature. Wood Sci Technol 19:159-177.

Becker P (2002) Modellierung des zeit- und feuchteabhängigen Materialverhaltens zur Untersuchung des Langzeitverhaltens von Druckstäben aus Holz (in German). Dissertation, Bauhaus-Universität Weimar.

Chassagne P, Bou-Said E, Jullien JF, Galimard P (2005) Three dimensional creep model for wood under variable humidity-numerical analyses at different material scales. Mech Time-Depend Mat 9:203-223. doi: 10.1007/s11043-005-9001-y

Dubois F, Randriambololona H, Petit C (2005) Creep in wood under variable climate conditions: Numerical modeling and experimental validation. Mech Time-Depend Mat 9:173-202. doi: 10.1007/s11043-005-1083-z

European Standard (2004) EN 302: Adhesives for load bearing timber structures - Tests methods - Part 1: Determination of longitudinal shear strength.

Fortino S, Mirianon F, Toratti T (2009) A 3D moisture-stress FEM analysis for time dependent problems in timber structures. Mech Time-Depend Mat 13:333-356. doi: 10.1007/s11043-009-9103-z

Furuno T, Saiki H, Goto T, Harada H (1983) Penetration of glue into the tracheid lumina of softwood and the morphology of fractures by tensile-shear tests. Mokuzai Gakkaishi 29:43-53.

Gereke T (2009) Moisture-induced stresses in cross-laminated wood panels. Dissertation, ETH Zurich.

Gereke T, Hass P, Niemz P (2010) Moisture-induced stresses and distortions in spruce cross-laminates and composite laminates. Holzforschung 64:127-133. doi: 10.1515/HF.2010.003

Gereke T, Niemz P (2010) Moisture-induced stresses in spruce cross-laminates. Eng Struct 32:600-606. doi: 10.1016/j.engstruct.2009.11.006

Gindl-Altmutter W, Mueller U, Konnerth J (2012) The significance of lap-shear testing of wood adhesive bonds by means of Volkersen's shear lag model. Eur J Wood Wood Prod 70:903-905. doi: 10.1007/s00107-012-0621-z

Grimsel M (1999) Mechanisches Verhalten von Holz (in German). Dissertation, Technische Universität Dresden.

Hanhijärvi A (1995) Modelling of creep deformation mechanisms in wood. Dissertation, Helsinki University of Technology.

Hass P, Wittel FK, Mendoza M, Herrmann HJ, Niemz P (2012) Adhesive penetration in beech wood: experiments. Wood Sci Technol 46:243-256. doi: 10.1007/s00226-011-0410-6

Hering S, Keunecke D, Niemz P (2012) Moisture-dependent orthotropic elasticity of beech wood. Wood Sci Technol 46:927-938. doi: 10.1007/s00226-011-0449-4

Kaliske M, Rothert H (1997) Formulation and implementation of three-dimensional viscoelasticity at small and finite strains. Comput Mech 19:228-239. doi: 10.1007/s004660050171

Keunecke D, Hering S, Niemz P (2008) Three-dimensional elastic behaviour of common yew and Norway spruce. Wood Sci Technol 42:633-647. doi: 10.1007/s00226-008-0192-7

Koch S (1996) Elastisches Kleben im Fahrzeugbau - Beanspruchungen und Eigenschaften (in German). Dissertation, Technische Universität München.

Konnerth J, Valla A, Gindl W (2007) Nanoindentation mapping of a wood-adhesive bond. Appl Phys A-Mater 88:371-375. doi: 10.1007/s00339-007-3976-y

Konnerth J, Gindl W, Mueller U (2007) Elastic properties of adhesive polymers. I. Polymer films by means of electronic speckle pattern interferometry. J Appl Polym Sci 103:3936-3939. doi: 10.1002/app.24434

Liu T (1993) Creep of wood under a large-span of loads in constant and varying environments .1. Experimental observations and analysis. Holz Roh Werkst 51:400-405. doi: 10.1007/BF02628237

Liu T (1994) Creep of wood under a large-span of loads in constant and varying environments .2. Theoretical investigations. Holz Roh Werkst 52:63-70. doi: 10.1007/BF02615022

Martensson A (1994) Creep-behavior of structural timber under varying humidity conditions. J Struc Eng-ASCE 120:2565-2582.

Moutee M, Fafard M, Fortin Y, Laghdir A (2005) Modeling the creep behavior of wood cantilever loaded at free end during drying. Wood Fiber Sci 37:521-534.

Müller U, Sretenovic A, Vincenti A, Gindl W (2005) Direct measurement of strain distribution along a wood bond line. Part 1: Shear strain concentration in a lap joint specimen by means of electronic speckle pattern interferometry. Holzforschung 59:300-306. doi: 10.1515/HF.2005.050

Ormarsson S (1999) Numerical analysis of moisture-related distortions in sawn timber. Dissertation, Chalmers University of Technology.

Ormarsson S, Dahlblom O, Petersson H (1998) A numerical study of the shape stability of sawn timber subjected to moisture variation - Part 1: Theory. Wood Sci Technol 32:325-334.

Ranta-Maunus A (1975) Viscoelasticity of wood at varying moisture-content. Wood Sci Technol 9:189-205.

Serrano E (2000) Adhesive joints in timber engineering - Modelling and testing of fracture properties. Dissertation, Lund University.

Serrano E (2004) A numerical study of the shear-strength-predicting capabilities of test specimens for wood-adhesive bonds. Int J Adhes Adhes 24:23-35. doi: 10.1016/S0143-7496(03)00096-4

Svensson S, Toratti T (2002) Mechanical response of wood perpendicular to grain when subjected to changes of humidity. Wood Sci Technol 36:145-156. doi: 10.1007/s00226-001-0130-4

Zink AG, Davidson RW, Hanna RB (1996) Finite element modeling of double lap wood joints. J Adhesion 56:217-228. doi: 10.1080/00218469608010509